A Comparison of Orthomosaic Software for Use with Ultra High Resolution Imagery of a Wetland Environment

John W. Gross [a]

[a] Center for Geographic Information Science and Geography Department, Central Michigan University, Mt. Pleasant, MI 48859

Abstract

Unmanned aerial systems are becoming popular in numerous military, civil, and research applications as a platform for the collection of ultra-high spatial resolution imagery in a cost-effective, dynamic manner. The use of unmanned aerial systems, however, requires significant CPU intensive pre-processing to convert hundreds of raw images into a single usable representation of the earth's surface. The goal of this study is to compare geometric accuracy, visual quality, ease of use and cost of Photoscan Pro, Pix4D Pro Mapper and Microsoft Image Composite Editor; three modern image stitching software packages which have the potential to significantly decrease the amount of time and user input required for creating orthomosaics. 223 usable images with spatial resolutions of 1.26 cm were collected on 26 September 2014 using an unmanned aerial system. Photoscan Pro, Pix4d Pro Mapper, and Image Composite Editor were used to create orthomosaics from the individual images. All orthomosaics were georeferenced using 54 ground control points collected during the field season. The geometric accuracy of the orthomosaics was calculated using the root mean square error of 17 validation points. Statistical analysis was used to examine the level of significance between the different software's. Microsoft Image Composite Editor had significantly fewer visual errors (Chi Square, $p < .001$) but, it had the poorest geometric accuracy with an RMSE of 34.7 cm (Tukey-Kramer, $p < 0.05$). Photoscan Professional had the most visual errors (Chi Square, $p < 0.001$), and an RMSE of 10.9 cm. Pix4D Pro had the best geometric accuracy with an RMSE of 7.7 cm, however this was not found to be statistically different from Photoscan (Tukey-Kramer, $p > 0.05$). These results suggest that there is no single best choice in terms of image stitching software, and that software selection must be made on the budget and geometric and visual quality requirements of the individual project.

1. Introduction

Unmanned aerial systems (UASs), have been used, in varying forms since the 1930's, primarily in military applications (http://www.science.smith.edu/cmet/safetycode/faq.html; Degarmo, 2004). Since the early 2000's, however, the possible capabilities of UAVs in civil applications such as biological research, precision agriculture, and archeology have become well documented (Knoth et al, 2013; Verhoeven 2011; Verhoeven 2012; Zhenkun et al, 2013). This growth will likely continue as government regulations and safety practices adapt to meet demands (Zweig et al., 2014). The primary use of UAS in civil applications is as a platform for the collection of ultra-high resolution (sub-decimeter) imagery. The use of such miniaturized platforms and consumer-grade sensor equipment, however, leads to the collection of hundreds of individual images which typically lack, or it exists but is of questionable accuracy, much of the ancillary information commonly used in traditional airphoto interpretation. This lack of accurate

information translates into the requirement for novel techniques to convert these hundreds of images into a single usable representation of the earth's surface.

Many UAS studies have utilized consumer grade available digital cameras (Laliberte et al, 2008).The use of such cameras combined with the small UAS platform can potentially create a number of problems. There can be significant variability in rotational and angular camera position, degree of overlap, and illumination (Barazzetti et al, 2010). The low flight altitude of the UAS in relation to changes in ground elevation can lead to significant perspective distortions (Zhang et al, 2011). Also, the global positions systems (GPS) and inertial measurement units on board the UAS are typically too inaccurate to be meaningful, leading to significant errors in the external operating parameters (EO) of the imagery (Laliberte et al, 2007; Turner et al, 2012). Such errors, combined with the large number of images, make conventional photogrammetric techniques difficult, if not impossible.

Recent advancements in the fields of photogrammetry and computer vision have produced a number of algorithms that have the potential to not only handle these issues, but to do so in a highly automated fashion. Such algorithms are able to detect and match hundreds of overlapping images, accurately estimate internal and external camera parameters, create point cloud representations of the 3D surface, and combine everything into a single, seamless 3D model or orthomosaic. One of the most notable sets of algorithms for this purpose is structure from motion (SfM). SfM is of benefit because it does not require a priori knowledge of any camera parameters or scene information (Choudhary, 2012; Westoby et al, 2012). SfM typically utilizes scale invariant feature transform (SIFT) to locate important features known as keypoints. SIFT locates keypoints in an image using a difference-of-Gaussian function (Lowe, 2004). Keypoints are then matched in each image based on the minimization of Euclidian distance (Lindeberg, 2012). These keypoints are then tracked from image to image enabling the accurate estimation of both camera orientation as well as keypoint location (Westoby et al, 2012). These keypoints become a dense cloud allowing for the construction of a 3D representation of the scene.

Previous research has utilized a variety of homemade SfM scripts to varying degrees of success. Laliberte et al. (2008) flew imagery over the Jornada Experimental Range in southern New Mexico. They used Autopano pro, a SIFT based software, to generate keypoints. These keypoints were included in a custom script known as PreSync which also incorporated a 1 m digital orthoquad and a 10 m digital elevation model to adjust and improve existing EOs. The original images as well as the updated EOs were then put into Leica Photogrammetric Suite to generate the mosaic. They were able to obtain overall RMSE of 47.9 cm which in part was due to a lack of differential correction on their GPS unit. Turner et al 2012 created an automated technique using SIFT and SfM techniques to automate the mosaicking of imagery collected over two sites of an Antarctic moss bed. They were able to achieve mean absolute total errors ranging from .103 m to 1.247 m.

Since 2010 a number of commercial SfM software packages have become available. Two of the most popular include Photoscan Professional (Photoscan), and Pix4D Mapper Pro (Pix4D). Both these software have been successfully used in current research (Vallet et al. 2011;

Kung et a.l 2011a; Kung et al. 2011b; Verhoeven et al.2011; Verhoeven et al. 2012; Woodget et al. 2014).

The goal of this research was to compare software packages for use with imagery acquired by UAS. Two commercially available Sfm software packages Photoscan and Pix4D were compared as well as Microsoft Image Composite Editor (ICE) a freeware available through Microsoft, which does not create a 3D point cloud, but rather stiches the images together directly. This analysis focused on four main components: ease of use, visual quality, geometric accuracy, and cost. Previous comparisons have reported that Photoscan Pro was the more accurate software based primarily on digital surface modeling results and not a quantitative analysis of image quality. (Sona et al. 2014; Turner et al. 2014),

2. Data

969 images were collected on 26 September 2014 at Braeburn Marsh Preserve near Ann Arbor Michigan, USA (~42° 16' N, ~84° 4'W). Imagery was collected using a Cannon EOS 6D digital single lens reflex camera with a 50mm fixed focal length lens at a flight of 100m.The camera was mounted on a Leptron Avenger airframe (Leptron, Golden, CO). All mission parameters and flight limits were monitored and controlled via a ground station using piccolo command center (Cloud Cap Technology, Hood River, OR). After the removal of low quality images and turns in the flight lines (which reduce the accuracy of the final product), only 224 images were retained for analysis, covering 15.5 acres with a spatial resolution of 1.26 cm. Due to the low accuracy of the camera GPS (25 m) no GPS EXIF data was retained for the analysis.

Ground control points (GCP) were established prior in the field season using a R8 GNSS RTK rover and a TCS3 hand held unit (Trimble Navigation Limited, Sunnyvale, California) with a recorded horizontal accuracy of +- 2 cm (95% confidence interval). Each point was marked with a metal pole and colored foam for easy recognition in the imagery. A total of 70 points were collected.

3. Methods

3.1 Overview

The 224 images, and 53 GCPs were used to create an image mosaic. The image mosaic was created using all three software packages; Photoscan Pro, Pix4D, and ICE. The resultant mosaics were then subjected to geometric and visual quality assessments and statistical analysis. A basic workflow of the methodology can be seen in figure 1.

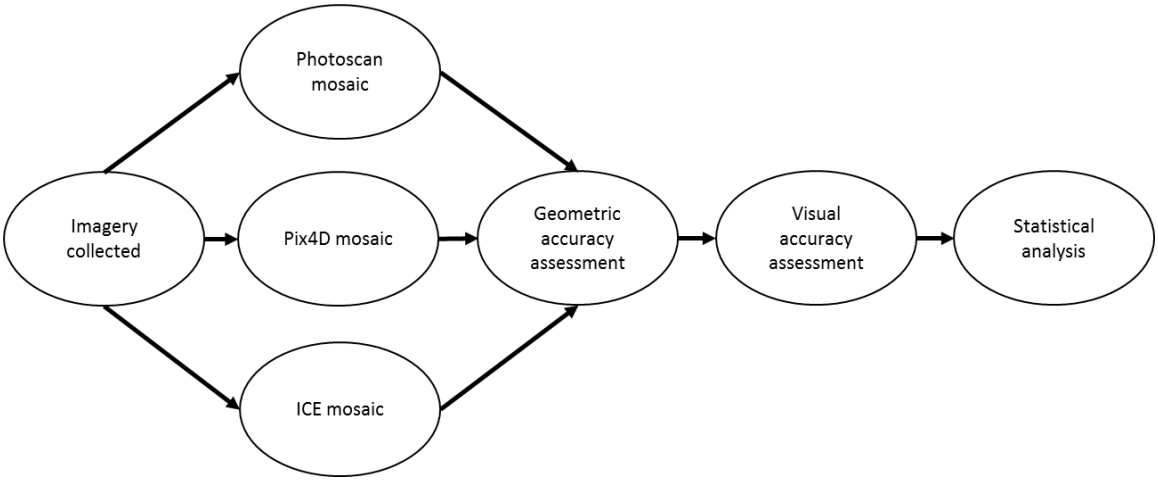

Figure 1: Basic workflow of methodology

3.2 Photoscan Pro

Created by the Russian based company Agisoft in 2010, Photoscan Pro is a 3D model and image stitching software package. It utilizes an adapted form of the popular structure from motion technology known as the scale invariant feature transformation proposed by Lowe (2004). At its core this process uses feature points, which are simply geometrically similar and distinct regions in an image e.g. building corners or the top of light posts. These points are then tracked across multiple images creating a series of connections between photographs (Verhoeven, 2011). In addition, this algorithm allows Photoscan Pro to automatically and accurately estimate a large number of internal and external camera parameters which previously had to be known and entered manually. Utilizing such algorithms, software packages such as Photoscan Pro are capable of matching images at the subpixel level (Woodget et al., 2014).

The Photoscan Pro workflow can be broken down into four basic steps: image alignment, dense point cloud formation, mesh creation, and texture creation. Each of these steps are run independent of each other, and aside from the inclusion of ground control points they can be run with little to no user input. It is also important to note that these stages are all independent and can be saved separately for later use or revision.

There are a number of parameters that must be defined, often with multiple options for each parameter. These parameters give the user control over a number of crucial factors that affect the overall quality of the final output, such as: the maximum number of tie-points to include in the cloud point, what type of surface the imagery consists of, and how to handle any gaps in the final model. Trial and error in combination with a careful review of user's manual was used to parametrize each step (. A complete list of the parameters can be seen in table 1.

Table 1: Parameter settings for Photoscan

Photoscan		
Step	**Parameter**	**Setting**
align photos	accuracy	high
	pair preselection	disabled
	point limit	40000
build dense pointcloud	quality	low
	depth filtering	mild
build mesh	surface type	height field
	source data	dense cloud
	polygon count	medium
	interpolation	enabled
build texture	mapping mode	adaptive orthophoto
	blending mode	mosaic
	texture size	4096

3.3 Pix4D

Pix4D is alternative orthomosaic software created in 2011 by a Swiss company of the same name. The Pix4D workflow consists of three steps: initial processing, point cloud densification, and DSM and orthomosaic generation. The user defined properties which guide the quality, accuracy, and format of the final output are all handled through a processing options dialogue box which must be set up prior to any processing steps. The options in this box refined into five sections: initial processing, point cloud, DSM orthomosaic, additional outputs, and resources. A complete list of the parameters can be seen in table 2.

Before any processing is done or parameters are set, Pix4D highly recommends the inclusion of any GCP data that may be available. This data is especially important since no GPS data was included in the EXIF data for the images. GCP data also helps reduce shift problems and other errors which may be present in the final model. Each of the GCPs was located in 5 of the images to help ensure image quality.

Table 2: Parameter settings for Pix4D

Pix4D		
Step	**Parameter**	**Setting**

initial processing	processing	aerial nadir
	feature extraction	1
	optimization	externals and all internals
	output	none selected
point cloud	image scale	1/4 (multiscale on)
	point density	optimal
	minimum number of matches	3
	point cloud filters	none
DSM/orthomosaic	noise filtering	on
	surface smoothing	on
	export type	geotiff
resources	resources	all available

3.4 Microsoft ICE

ICE is an advanced panoramic image stitcher freeware produced by Microsoft typically used to create detailed panoramas from numerous individual images. Unlike the other software packages, ICE does not create a separate 3D point cloud and cannot generate 3D images. For these reason, and because it is not designed to be used in scientific research, it does not create the same number of outputs as Photoscan and Pix4D (i.e. no dense point clouds or meshes).Therefore number of steps and parameters is relatively limited. In addition ICE currently has no way to implicitly include GCPs in program. ICE is run in 4 sequential steps: import, stitch, crop (optional) and export. A complete list of the parameters can be seen in table 3.

Table 3: Parameter settings for ICE

ICE		
Step	**Parameter**	**Setting**
import	panorama type	simple
	camera motion	auto-detect (planar)
stitch	roll	0 degrees
export	scale	100
	file format	JPEG
	quality	100/high

3.5 Geometric Accuracy Assessment

To quantify geometric accuracy, root mean square error (RMSE) was used. RMSE is the comparison of real world (ground truth) information to estimated (image derived) measurements. In the case of this research 17 GCPs had their real world location compared to their estimated location in all orthomosaics. RMSE calculations were conducted using the following equation:

$$\sqrt{\frac{\sum_{i=1}^{n}\left(\left(X_i - X_{i,measured}\right)^2 + \left(Y_i - Y_{i,measured}\right)^2\right)}{n}} \qquad \text{eq. (1)}$$

where n is the total number of samples, X_i and Y_i are the X and Y measurements of point i's location in the image, and $X_{i,measured}$ and $Y_{i,measured}$ are the position of GCP i as measured in the field. To determine statistical significance a one way stacked ANOVA was conducted in MINITAB (version 14) with $\alpha = 0.05$. Although the data was not normally distributed ANOVA was still conducted because ANOVA is not very sensitive to deviations from normality, and is more powerful than the Kruskal-Wallis test (McDonald, 2014). Contingent on the results of the ANOVA post hoc Tukey-Kramer test were also conducted for each pairwise comparison.

3.6 Visual Quality Assessment

To quantify the visual quality of the images, 100 points were created using the 'create random points' tool in ArcGIS 10.2.2. A 2.5 m (5 m diameter) circular buffer was created around each point. These locations were then assigned to one of four landcover classes based on visual interpretation: reed canary grass (RCG), typha marsh (TM), wet-mesic prairie (WMP), or woody vegetation (WV). A binary classifier (1 or 0) was used to denote the presence of image artifacts and image blur. Chi Square tests for independence were calculated between image groups (i.e. Pix4D vs ICE), and Fishers exact tests were used within image groups (Pix4D WV vs Pix4D TM) with Bonferroni corrections applied as necessary (McDonald, 2014).

4. Results and Discussion

4.1 Geometric Accuracy

The results of this analysis are found in figure 2 and table 4. Overall Pix4D had the highest level of geometric accuracy (RMSE = 7.7 cm) compared to Photoscan (RMSE = 10.9 cm) and ICE (RMSE = 34.7 cm). Pix4D and Photoscan were found to be statistically significantly better than ICE ($p < 0.05$), however, they were not statistically different from each other ($p > 0.05$) (table 4). This is readily apparent when the x and y errors are viewed graphically, as ICE has much greater errors in both the x and y direction (figure 2). It should be noted that a certain amount of the increased error of Photoscan relative to Pix4D may be due in part to the increased presence of image artifacts which made it more difficult to accurately determine the geometric centers of the GCPs.

The accuracies achieved by Photoscan Pro and Pix4d are comparable to values reported in previous literature using UAS imagery. For example, a study conducted in 2010 by Laliberte et al found RMSE values of 11.95 cm, 20.17 cm, and 16.69 cm for images collected over three study sites in southwestern Idaho.

Table 2: Tukey test results for geometric accuracy assessment. ANOVA p value = 0.001 **Bold** values indicate significance

	Lower Boundary	Center	Upper Boundary
ICE vs Photoscan	**-0.187**	**-0.108**	**-0.030**
ICE vs Pix4D	**-0.193**	**-0.114**	**-0.036**
Pix4D vs Photoscan	-0.084	-0.006	0.072

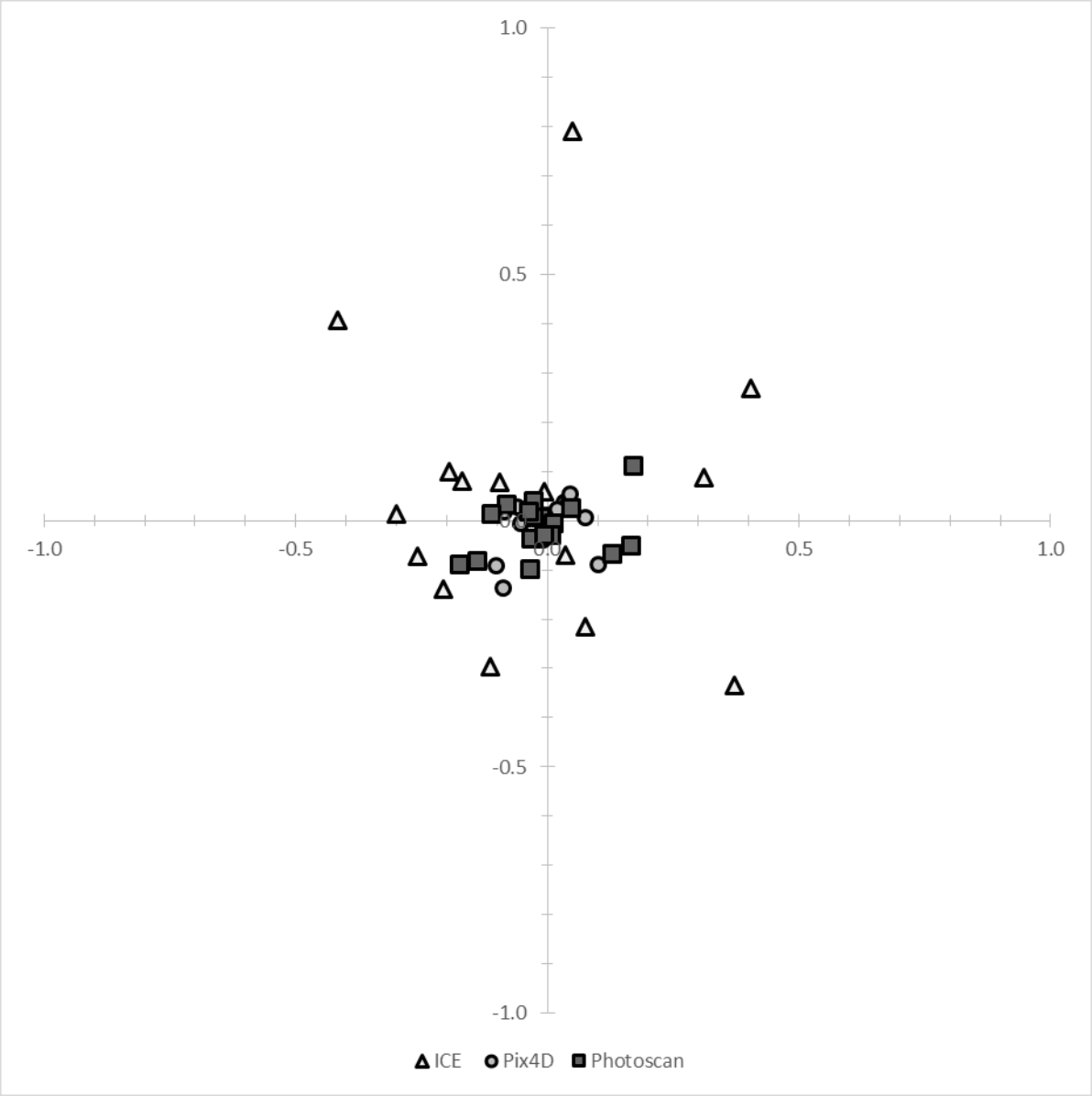

Figure 2: Geometric error in the x and y direction for the 17 validation points

4.2 Visual Quality

The results of this analysis are shown in figures 3 & 4 and tables 5, 6 and 7. Photoscan had significantly more image artifacts ($p < 0.001$) with 89% of the sites showing some degree of artifacts (figure 3). Photoscan also had the highest proportion of image artifacts in each class, with p values less than .001 in all comparisons (table 5). ICE did not produce any image artifacts in any of the sites (figure 3). The only class comparison which was not found to be significant was the comparison of wet-mesic prairie in ICE vs Pix4D ($p = 0.306$). The p value of typha marsh between ICE and Pix4D ($p = 0.019$) was considered significant due to its proximity with

regards to the target value and the documented conservative nature of Bonferroni corrections (McDonald, 2014).

Pix4D had the highest overall incidences of image blur with 38% of the total sites (figure 4). Pix4D was found to be overall statically significantly different from Photoscan ($p < 0.001$) and ICE ($p = 0.005$) but, ICE was not found to be significantly different from Photoscan ($p = 0.259$) (table 6). Additionally, most of the within class comparisons were found to statistically insignificant (table 6).

Woody vegetation had the highest percentages of both image blur and artifacts across all three mosaics (figures 3 & 4). However, there was no statically significant difference found between the classes with regards to the proportion of sites with artifacts in any of the mosaics. Only the woody vegetation was found to be statistically significant from the other classes in Photoscan and Pix4D with regards to image blur (table 7). Again, the p value of 0.017 was considered significant due to the conservative nature of Bonferroni corrections. One potential cause of the increased number of sites with image blur and artifacts found in woody vegetation is the increased presence of windblown leaf movement occurring in the canopies between flight lines. This relative shift in location between images compared to other more stable targets, may increase the difficulty of matching those portions of the images.

*Table 5: p values for each class in terms of image artifacts compared between the three mosaics. Value in parenthesis is the target p value for the column after Bonferroni corrections **bold** values are significant. * indicates potential false negative.*

Class	ICE vs Photoscan vs Pix4D (p=0.050)	ICE vs Photoscan (p=0.017)	ICE vs Pix4D (p=0.017)	Photoscan vs Pix4D (p=0.017)
Overall	**< 0.001**	**< 0.001**	**< 0.001**	**< 0.001**
Reed canary grass	**< 0.001**	**< 0.001**	**< 0.001**	**< 0.001**
Wet-mesic prairie	**< 0.001**	**< 0.001**	0.306	**0.001**
Typha marsh	**< 0.001**	**< 0.001**	**0.019***	**0.001**
Woodland Vegetation	**< 0.001**	**< 0.001**	**< 0.001**	**< 0.001**

*Table 6: p values for each class in terms of image blur compared between the three mosaics. Value in parenthesis is the target p value for the column after Bonferroni corrections **bold** values are significant. NA represent comparisons that was not calculated because overall comparison was not significant or did not have enough data.*

Class	ICE vs Photoscan vs Pix4D (p=0.050)	ICE vs Photoscan (p=0.017)	ICE vs Pix4D (p=0.017)	Photoscan vs Pix4D (p=0.017)
Overall	**< 0.001**	0.259	**0.005**	**< 0.001**
Reed canary grass	**0.040**	0.040	0.585	**0.011**
Wet-mesic prairie	0.192	NA	NA	NA
Typha marsh	0.081	NA	NA	NA
Woodland Vegetation	**0.001**	0.397	**0.001**	**0.007**

*Table 7: p values for each class comparison in terms of image blur. Value in parenthesis is the target p value for the column after Bonferroni corrections **bold** values are significant. * indicates potential false negative. NA represent data that was not calculated because overall comparison was not significant or did not have enough data.*

class	ICE (0.008)	Pix4D (0.008)	Photoscan (0.008)
overall	0.065	**< 0.001**	**< 0.001**
canary reed grass vs wet-mesic prairie	NA	0.399	1.000
canary reed grass vs typha marsh	NA	0.550	1.000
canary reed grass vs woody vegetation	NA	**< 0.001**	**0.001**
wet-mesic prairie vs typha marsh	NA	1.000	1.000
wet-mesic prairie vs woody vegetation	NA	**0.003**	**0.017***
typha marsh vs woody vegetation	NA	**< 0.001**	**0.002**

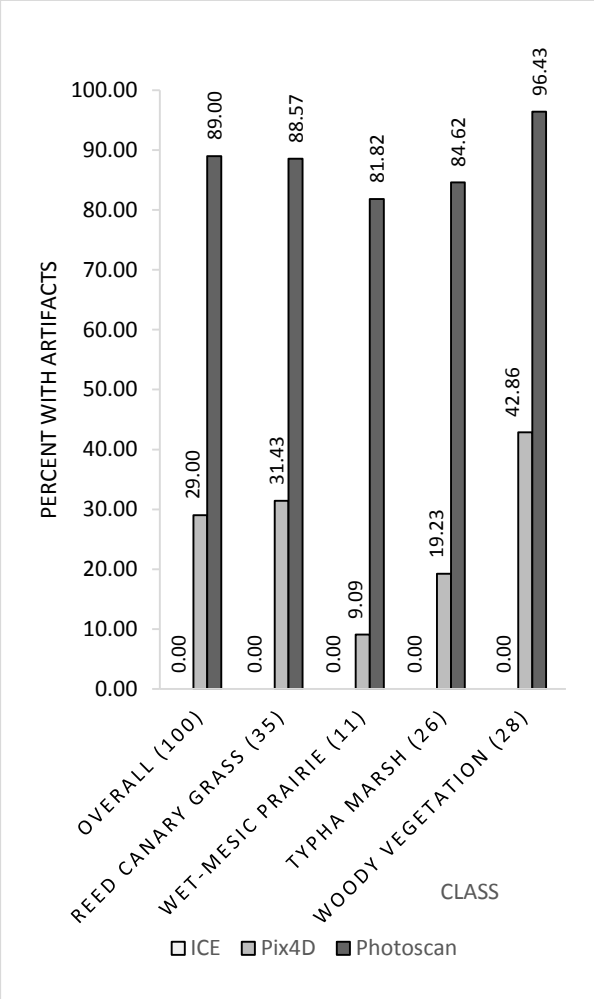

Figure3: percent of each class with image artifacts

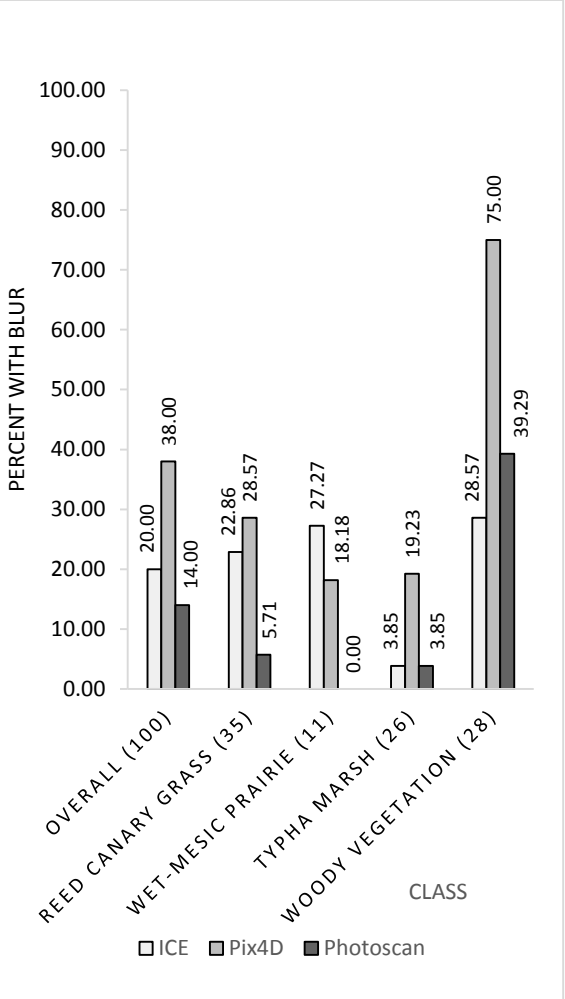

Figure 4: percent of each class with image blur

4.3 Cost

Although ICE is a freely available download from Microsoft, it does not have the same features as the other software, namely 3D surface modeling. However, Installation is easy and expandable without complicated licensing software. In terms of the commercial SfM software packages, Photoscan is significantly cheaper, costing only $549 for an educational license. Comparatively Pix4D costs $4,990 for a non-commercial license. A less expensive option is available, however, it has stringent requirements on publication processes and requires yearly update reports with regards to use. Pix4D does offer license rentals at monthly or yearly rates of $350 and $8,700 respectively, however, no educational discounts are available for these rates. It is also important to note that Pix4D includes a second license specifically designated to using the rapid check functionality in the field to verify data accuracy.

4.4 Ease of Use

ICE's user interface (UI) was the simplest of the three programs, due in part to the fact that it does not generate a 3D point cloud. Many of its parameters consist of slid bars, which

make adjustments simple. With only a single processing step, ICE offers the least amount of control over the workflow. Additionally, it does not possess any in program GCP placement UI, meaning that third party software such as ENVI or ArcGIS is required to georeference the resulting mosaic.

Overall the UI of Photoscan was clean and user friendly. Images could be easily added, disabled, and removed at any point in the workflow. Each step could be run and saved independently making it much easier to adjust settings of individual steps to achieve the best results. Multiple GCPs could be placed in one image at a time, and have their location predicted, significantly reducing time and effort when placing GCPs, which is the most user intensive step of the process. Photoscan also offers an easy to use batch processing mode, which allows users to chain together any functionality, set parameters, and run them as one process.

Pix4D offered the most complicated UI. Included in its UI is a basemap image allowing for an in program comparison of GCPs and mosaics to the real world prior to export. Unfortunately, this can, at times, make viewing the finished mosaic in program slightly cumbersome. In contrast to Photoscan's modular setup, Pix4D has all its parameters set up in advance using a single options menu. The initial processing, point cloud densification, and DSM/Orthomosaic creation can then be run independently or all handled in a single execution. Pix4D highly recommends the inclusion of GCP data not only to georeference the final outputs, but also to help avoid a number of common errors, such as inverted mosaics. Pix4D's UI for GCP placement, however, uses small sub windows within the layout and requires significant time and energy to implement (approx. 8 hours for 52 GCPs with 5 images each), compared to Photoscan (approx. 4 hours).

5. Conclusion

With the use of UAS increasing both in the academic and civil sectors it is important to find quick, accurate methods for converting significant numbers of images into a single usable orthomosaic. This research has presented three possible alternative software packages which offer a highly automated approach, Photoscan Pro, Pix4D, and Microsoft Image Composite Editor. A summary of the findings can be seen in table 8. Although, Photoscan Pro and Microsoft Image Composite Editor were easier to use than Pix4D, Photoscan proved to be least effective in terms of visual accuracy, and ICE had the worst geometric accuracy. In addition all three software packages struggled with tree canopies where windblown leaf movement led to increased numbers of image artifacts or blur. Therefore, this research suggests that there is no single best option for optimizing all criteria, and a software selection should reflect the cost/benefit trade off between cost, ease of use, geometric accuracy, and visual quality for the individual application.

Table8: Overall comparison between the software. Numbers represent the software order for that category with 1 being the highest. Duplicate values were awarded in cases where no statistical difference was observed

	Geometric accuracy	Visual quality	Cost	Ease of use
ICE	2	1	1	2
Photoscan Pro	1	3	2	1
Pix4D	1	2	3	3

6. Acknowledgements and Funding

This research was funded by the Center for Geographic Information Science at Central Michigan University. Without the help of Dr. Benjamin Heumann, Rachel Hackett, Brian Stark, and Sam Lipscomb with regards to data collection this project would not have been possible. In addition, a special thanks is given to Braeburn Nature Preserve for allowing us frequent access to the site.

7. References

Barazzetti, L., F. Remondino, M. Scaioni, and R. Brumana. 2010. Fully automatic UAV image-based sensor orientation.*in* Proceedings of the 2010 Canadian Geomatics Conference and Symposium of Commission I.

Choudhary, S., and P. Narayanan. 2012. Visibility probability structure from sfm datasets and applications. Pages 130-143 Computer Vision–ECCV 2012. Springer.

DeGarmo, M. T. 2004. Issues concerning integration of unmanned aerial vehicles in civil airspace. The MITRE Corporation Center for Advanced Aviation System Development.

Knoth, C., B. Klein, T. Prinz, and T. Kleinebecker. 2013. Unmanned aerial vehicles as innovative remote sensing platforms for high-resolution infrared imagery to support restoration monitoring in cut-over bogs. Applied Vegetation Science **16**:509-517.

Küng, O., C. Strecha, A. Beyeler, J.-C. Zufferey, D. Floreano, P. Fua, and F. Gervaix. 2011a. The accuracy of automatic photogrammetric techniques on ultra-light UAV imagery.*in* UAV-g 2011-Unmanned Aerial Vehicle in Geomatics.

Küng, O., C. Strecha, P. Fua, D. Gurdan, M. Achtelik, K.-M. Doth, and J. Stumpf. 2011b. Simplified building models extraction from ultra-light uav imagery. ISPRS-International Archives of the Photogrammetry, Remote Sensing and Spatial Information Sciences **3822**:217.

Laliberte, A. S., J. E. Herrick, A. Rango, and C. Winters. 2010. Acquisition, orthorectification, and object-based classification of unmanned aerial vehicle (UAV) imagery for rangeland monitoring. Photogrammetric Engineering & Remote Sensing **76**:661-672.

Laliberte, A. S., A. Rango, and J. Herrick. 2007. Unmanned aerial vehicles for rangeland mapping and monitoring: a comparison of two systems.*in* ASPRS Annual Conference Proceedings.

Laliberte, A. S., C. Winters, and A. Rango. 2008. A procedure for orthorectification of sub-decimeter resolution imagery obtained with an unmanned aerial vehicle (UAV). Pages 08-047 *in* Proc. ASPRS Annual Conf.

Lindeberg, T. 2012. Scale invariant feature transform. Scholarpedia **7**:10491.
Lowe, D. G. 2004. Distinctive image features from scale-invariant keypoints. International journal of computer vision **60**:91-110.
McDonald, J. H. 2009. Handbook of biological statistics. Sparky House Publishing Baltimore, MD.
Sona, G., L. Pinto, D. Pagliari, D. Passoni, and R. Gini. 2014. Experimental analysis of different software packages for orientation and digital surface modelling from UAV images. Earth Science Informatics **7**:97-107.
Turner, D., A. Lucieer, and L. Wallace. 2014. Direct georeferencing of ultrahigh-resolution uav imagery.
Turner, D., A. Lucieer, and C. Watson. 2012. An automated technique for generating georectified mosaics from ultra-high resolution unmanned aerial vehicle (UAV) imagery, based on structure from motion (SfM) point clouds. Remote Sensing **4**:1392-1410.
Verhoeven, G. 2011. Taking computer vision aloft–archaeological three-dimensional reconstructions from aerial photographs with photoscan. Archaeological Prospection **18**:67-73.
Verhoeven, G., M. Doneus, C. Briese, and F. Vermeulen. 2012. Mapping by matching: a computer vision-based approach to fast and accurate georeferencing of archaeological aerial photographs. Journal of Archaeological Science **39**:2060-2070.
Westoby, M., J. Brasington, N. Glasser, M. Hambrey, and J. Reynolds. 2012. 'Structure-from-Motion'photogrammetry: A low-cost, effective tool for geoscience applications. Geomorphology **179**:300-314.
Woodget, A., P. Carbonneau, F. Visser, and I. Maddock. 2014. Quantifying submerged fluvial topography using hyperspatial resolution UAS imagery and structure from motion photogrammetry. Earth Surface Processes and Landforms.
Zhang, Y., J. Xiong, and L. Hao. 2011. Photogrammetric processing of low-altitude images acquired by unpiloted aerial vehicles. The Photogrammetric Record **26**:190-211.
Zhenkun, T., F. Yingying, and L. Suhong. 2013. Rapid crops classification based on UAV low-altitude remote sensing. Transactions of the Chinese Society of Agricultural Engineering **2013**.